

Utah State University

DigitalCommons@USU

Space Dynamics Laboratory Publications

Space Dynamics Laboratory

5-15-1997

Focus Optimization of the SPIRIT III Radiometer

Joseph J. Tansock

Andrew L. Shumway

Follow this and additional works at: https://digitalcommons.usu.edu/sdl_pubs

Recommended Citation

Tansock, Joseph J. and Shumway, Andrew L., "Focus Optimization of the SPIRIT III Radiometer" (1997).
Space Dynamics Laboratory Publications. Paper 155.
https://digitalcommons.usu.edu/sdl_pubs/155

This Article is brought to you for free and open access by the Space Dynamics Laboratory at DigitalCommons@USU. It has been accepted for inclusion in Space Dynamics Laboratory Publications by an authorized administrator of DigitalCommons@USU. For more information, please contact digitalcommons@usu.edu.



Focus optimization of the SPIRIT III radiometer

Joseph J. Tansock, MEMBER SPIE
Andrew L. Shumway, MEMBER SPIE
Utah State University
Space Dynamics Laboratory
1695 North Research Park Way
North Logan, Utah 84341
E-mail: joe.tansock@sdl.usu.edu

Abstract. The spatial infrared imaging telescope (SPIRIT III) radiometer is the primary instrument aboard the Midcourse Space Experiment (MSX), which was launched on April 24, 1997. The Space Dynamics Laboratory at Utah State University (SDL/USU) developed and implemented a ground-based procedure to optimize the focus of the SPIRIT III radiometer. The procedure used point source data acquired during ground measurements. These measurements were obtained with a calibration source consisting of an illuminated pinhole near the focus of a cryogenically cooled collimator. Simulated point source measurements were obtained at multiple focus positions by translating the pinhole along the optical axis inside and outside the optimum focus of the collimator. The radiometer was found to be slightly out of focus, and the detector focal plane arrays were moved to positions indicated by the test results. This method employed a single cryogenic cycle to measure both the distance and direction needed to adjust each array for optimal focus. The results of the SPIRIT III on-orbit stellar point source observation demonstrate the success of the technique. The method and hardware used to achieve focus optimization are described. © 1997 Society of Photo-Optical Instrumentation Engineers. [S0091-3286(97)00511-4]

Subject terms: infrared radiometric sensor calibration; infrared telescope; cryogenic focus; optical model; wavefront error.

Paper RSC-05 received May 15, 1997; revised manuscript received July 1, 1997; accepted for publication July 7, 1997. This paper is a revision of a paper presented at the SPIE conference on Infrared Spaceborne Remote Sensing V, August 1997, San Diego, CA. The paper presented there appears (unrefereed) in SPIE Proceedings Vol. 3122.

1 Introduction

The spatial infrared imaging telescope (SPIRIT III) sensor is the primary instrument on the Midcourse Space Experiment (MSX) satellite, which was launched into orbit on April 24, 1996. The Space Dynamics Laboratory at Utah State University (SDL/USU) designed, built, and calibrated SPIRIT III. The sensor consists of an off-axis reimaging telescope with a 35-cm-diam unobscured aperture, a six-band scanning radiometer, a six-channel Fourier transform spectrometer, a cryogenic Dewar/heat exchanger, and instruments to monitor contamination levels and their effects on the sensor.^{1,2}

The SPIRIT III radiometer consists of a high off-axis rejection telescope, scan mirror, spectral beamsplitters and filters, and five focal plane detector arrays located in the radiometer assembly. Each array, designated A through E, is spectrally filtered to a unique passband between 4 and 28 μm and contains 192 rows and a varying number of columns (two to eight) of active impurity band conductor, blocked impurity band (IBC/BIB) arsenic-doped silicon detectors. The detectors are mounted to field-effect transistor (FET), low-noise, cryogenic readout circuits. The radiometer assembly optics, shown in Fig. 1, reimage energy onto the arrays using reimaging mirrors M5 and M6, dichroic beamsplitters to split the incoming light into spectral bands, and filters over the arrays to select a spectral bandpass for each array. Arrays A and B, C and D, and E are individu-

ally collocated in the radiometer assembly. The scan mirror can scan or stop in either of the radiometer's two modes of operation: mirror-scan mode or earthlimb mode. The focal length of the radiometer is approximately 52.5 in.

SDL/USU developed a ground-based method to optimize the focus of each collocated array in the SPIRIT III radiometer. This method employed focus measurements, which consist of point source data acquired with the second-generation multifunction IR calibrator (MIC2). The point source data were obtained through a pinhole aperture near the focus of the MIC2. Simulated point source measurements were obtained at multiple focus positions by translating the pinhole along the optical axis inside and outside the MIC2's optimum focus. The focus of the MIC2 was then related to the focus of the radiometer using a scale factor equal to the square of the ratio of focal lengths of both the radiometer and the MIC2. Ensquared energy and full width at half maximum (FWHM) were evaluated as a function of focus position to determine optimum focus. The radiometer was found to be slightly out of focus, and the arrays were moved to positions given by the test results. This method provided both the distance and direction needed to adjust the focus of each array using data collected during a single cryogenic cycle. This paper describes the hardware, measurements, point response function, figures of merit, and optical modeling used to achieve focus optimization. Results of a SPIRIT III on-orbit stellar point

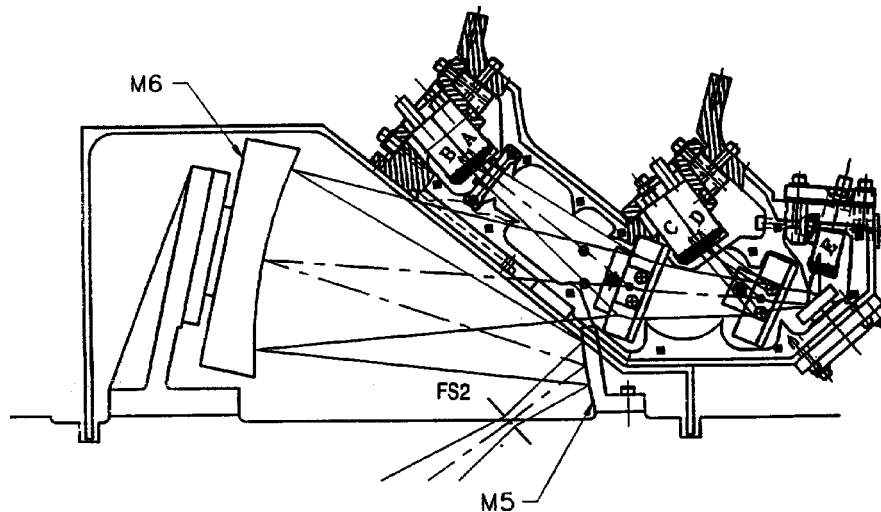


Fig. 1 Radiometer focal plane assembly.

source observation are given to demonstrate the success of this technique.

2 Measurement Hardware

The MIC2, designed and built by SDL/USU, combines multiple source configurations in a single cryogenically cooled IR calibrator.^{3,4} The optics are cooled to cryogenic temperatures using liquid helium contained in an internal cryogen holding tank. In collimator mode, the MIC2 provides a distant, small-area, full-entrance-aperture source through an off-axis Gregorian telescope with an effective focal length of 200 in., as illustrated in Fig. 2.

Optimizing the focus of the SPIRIT III radiometer depended on the focus of the MIC2. Therefore, SDL/USU performed interferometric measurements of the MIC2 to optimize its focus and characterize its wavefront errors.⁵ For focus evaluation, the cryogenic temperature antechamber (CTA) with the focus tester assembly (Fig. 3) were mounted to the MIC2 entrance port. This test was performed during an engineering evaluation cold test of the

SPIRIT III telescope. By closing a gate valve at the MIC2 entrance port, the exterior vacuum window plate was replaced with the CTA and focus tester assembly. The CTA was pumped and leak checked, and the focus tester assembly was cooled with liquid helium. The gate valve was then opened to create a common vacuum between the MIC2 and the CTA. A mechanical carriage was used to move the focus tester probe inside and outside the MIC2 focus along the optical axis. The pinhole aperture and IR source in the probe tip thus temporarily replaced the stationary MIC2 aperture with a movable aperture.

The focus tester IR source and 100- μm pinhole aperture, shown in Fig. 4, are positioned near the MIC2 aperture slide. The IR source is a small incandescent bulb coated with an epoxy and molybdenum disulfide mixture for a more spatially and spectrally uniform IR emission. A G10 thermal isolator supports the bulb and temperature diode mounted just behind the bulb. The bulb is capable of 300 K operation, while the probe's aluminum housing temperature

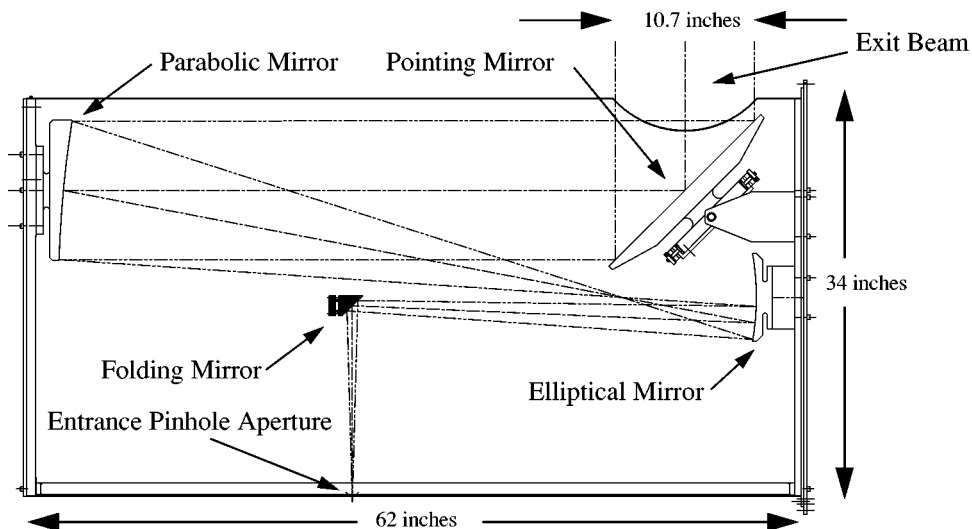


Fig. 2 MIC2 ray trace from pinhole entrance aperture to exit beam.

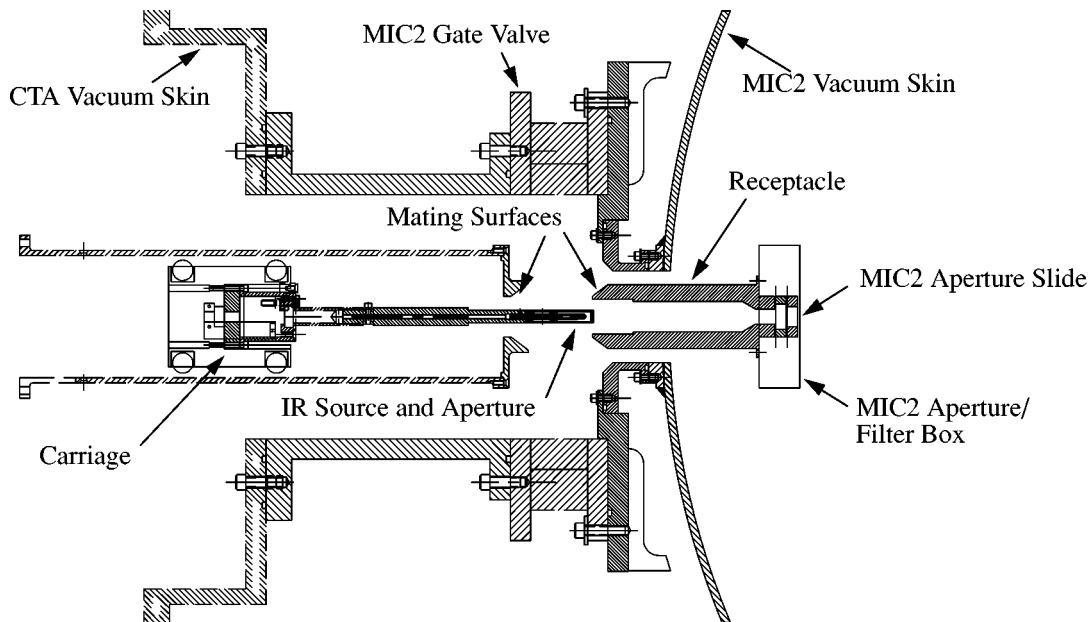


Fig. 3 CTA and focus tester assembly interfaced with the MIC2 entrance port. The focus tester assembly is shown in retracted position.

is 30 K. Thus, good temperature contrast is maintained between the pinhole and the bulb.

3 Methods

3.1 Focus Measurement

The aperture position of the focus tester probe relative to the MIC2 aperture slide was established by setting the MIC2 aperture slide to a partially open position and placing the probe in contact with the edge of the aperture slide. This position provided the distance from the probe aperture and the MIC2 aperture. To verify this mechanical position, the probe's pinhole aperture was simultaneously viewed by the radiometer. After centering the MIC2 aperture slide on the open position, the probe was then free to move along the optical axis of the MIC2.

To measure the optimum focus of the focal plane arrays, the probe's illuminated pinhole aperture was positioned at 15 focus positions along the MIC2 optical axis. The range of focus positions for the probe was approximately 1.8 in. centered near the MIC2 aperture. The MIC2 focus, defined

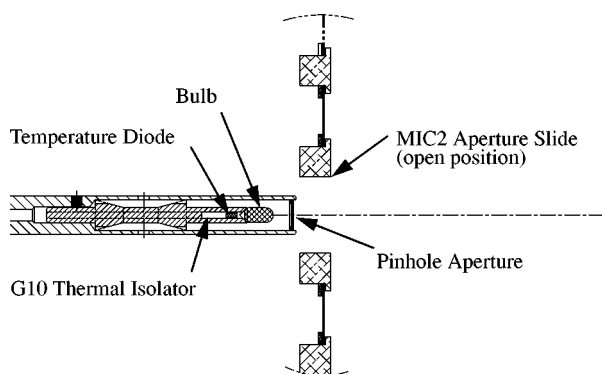


Fig. 4 Focus tester probe alignment with the MIC2 aperture slide.

by the position of the probe, was related to the SPIRIT III focus by multiplying the MIC2 focus position by the square of the ratio of the focal lengths of the MIC2 and the radiometer. Effectively, this method gives a range of radiometer focus positions of approximately 0.12 in.

For each focus position, the radiometer's response to the probe's 100- μm pinhole aperture, effectively a 20- μm source when viewed through the MIC2 optics, was measured in a 3 \times 3 grid pattern over the SPIRIT III field of regard. Two scans were collected at each of the 3 \times 3 point source grid positions in the field of regard.

3.2 Point Response Function

The point response function (PRF) is the radiometer's peak normalized response to a point source. The shape and size of the PRF is a function of focus (i.e., the smallest PRF is observed at the optimum focus). To generate the PRFs from the radiometer data, focal plane coordinate images were generated using the Gamma version of the SPIRIT III Convert software.⁶ Figure 5 shows the measured PRF for defocus values of -0.072, +0.004, and +0.051 in. for array A near the center of the field of regard. The optimum focus is shown when Δf is approximately 0.00 in., where the PRF is smallest and symmetrical. The astigmatism of the system is seen by observing the sagittal or tangential elongation of the PRF for the defocused results.

3.3 PRF Figures of Merit

Two PRF figures of merit, FWHM and 90- μrad energy density, were calculated using the measured PRFs from the focus test. The energy density was calculated by dividing the sum response inside a 90- μrad square by the total sum response. The FWHM was determined by calculating the in-scan and cross-scan width of the PRF at half peak response. As an example, Fig. 6 shows these figures of merit as functions of focus position for array C. The FWHM is

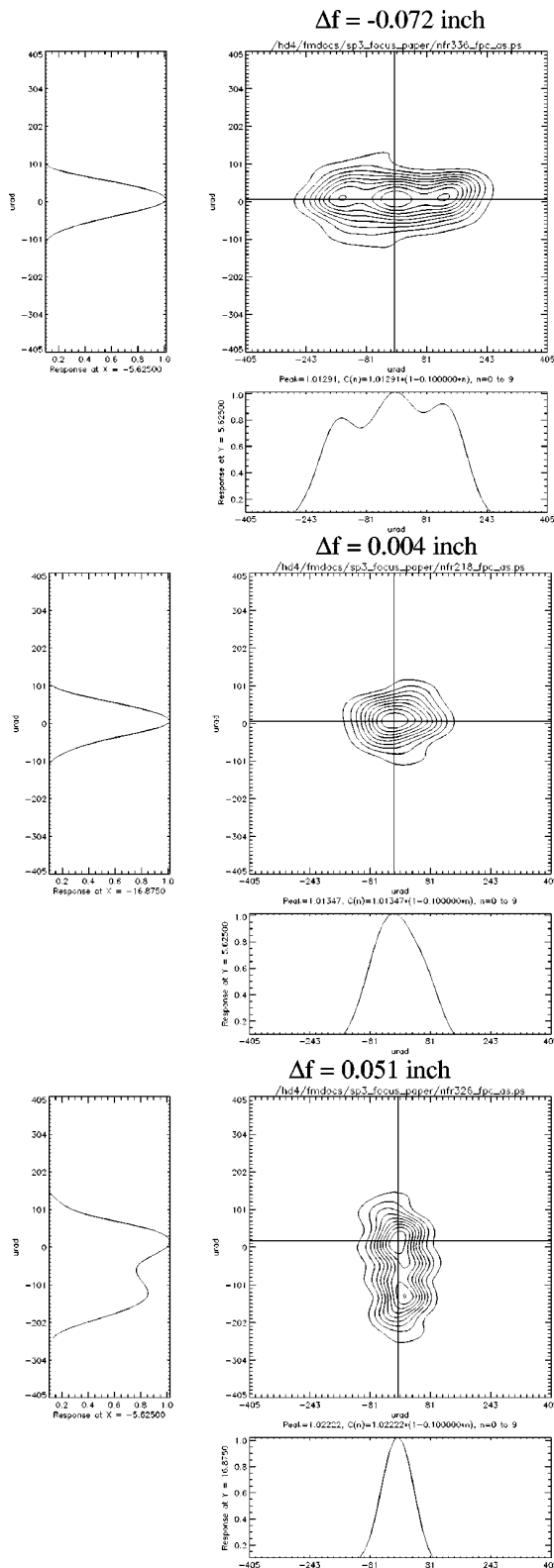


Fig. 5 Example focus test point response functions for three focus positions.

expressed as units of a $90\text{-}\mu\text{rad}$ detector (i.e., FWHM of 1 is equal to $90\text{ }\mu\text{rad}$). The lines that pass through the data were calculated from a cubic polynomial least-squares curve fit, and 0 on the horizontal axis is equal to the MIC2

infinity focus position. The FWHM and energy density figures of merit are related to each other but are not necessarily optimized at the same focus position. As shown by Fig. 6, the optimum focus of FWHM (i.e., symmetry) is optimized 0.006 in. to the right of the peak $90\text{-}\mu\text{rad}$ energy density.

3.4 Optical Modeling

To investigate how the image quality of the MIC2 may have affected the measured PRFs, system-level interferometric measurements were applied to an aberration-free optical model of the MIC2 and SPIRIT III using OSLO optical design software.⁷ The value of coupling interferometric measurements with optical design analysis was demonstrated by Willey and Patchin.⁸ SDL/USU performed interferometric measurements of the MIC2 collimator⁵ and Sensor Systems Group (SSG), the telescope vendor, performed interferometric measurements on the telescope.⁹ The interferograms were digitized and fit with Zernike polynomials to characterize the system wavefront error. The wavefront errors were scaled to $\lambda = 12\text{ }\mu\text{m}$ and added to the optical model using the Zernike surface option in OSLO. Because the entrance pupil of SPIRIT III was overfilled in one axis and underfilled in the other by the MIC2 exit pupil, models of the MIC2 exit pupil and SPIRIT III entrance pupil were included in the optical model. Figure 7 shows a schematic relationship of the MIC2-SPIRIT III optical model.

The focal plane of the SPIRIT III model was translated $\pm 0.04\text{ in.}$ with an increment of 0.01 in. along the optical axis to simulate defocus. For each defocus position, the point spread function was calculated using the optical model. These point spread functions were used to calculate FWHM and $90\text{-}\mu\text{rad}$ ensquared energy. These figures of merit are plotted as a function of defocus position in Fig. 8, which indicates that symmetry occurs 0.0076 in. outside focus, while the ensquared energy peaks at focus. This phenomenon parallels the figure of merit plot of the SPIRIT III focus measurements (Fig. 6), which also shows symmetry at 0.006 in. outside the focus that gives the maximum ensquared energy density.

To characterize the optimum focus of SPIRIT III while it views a stellar point source, the MIC2 model was removed from the optical model and replaced with an ideal point source near infinity. Again, the focal plane of the SPIRIT III model was translated to simulate defocus and point spread functions were calculated. The model results of FWHM and $90\text{-}\mu\text{rad}$ ensquared energy as a function of defocus for SPIRIT III viewing a star are shown in Fig. 9. The results show symmetry and peak ensquared energy occurring at the same focus position. These results suggest that the MIC2 image quality biased the focus position determined by the PRF symmetry. For this reason, radiometer focus was optimized using the $90\text{-}\mu\text{rad}$ ensquared energy figure of merit.

4 Focus Optimization

The peak $90\text{-}\mu\text{rad}$ energy density was used to set the optimum focus of the radiometer. Because the top, middle, and bottom of the arrays were found to be at a slightly different focus, the peak energy density focus positions at these locations were averaged to give an optimum focus position for each array. The radiometer assembly design enabled

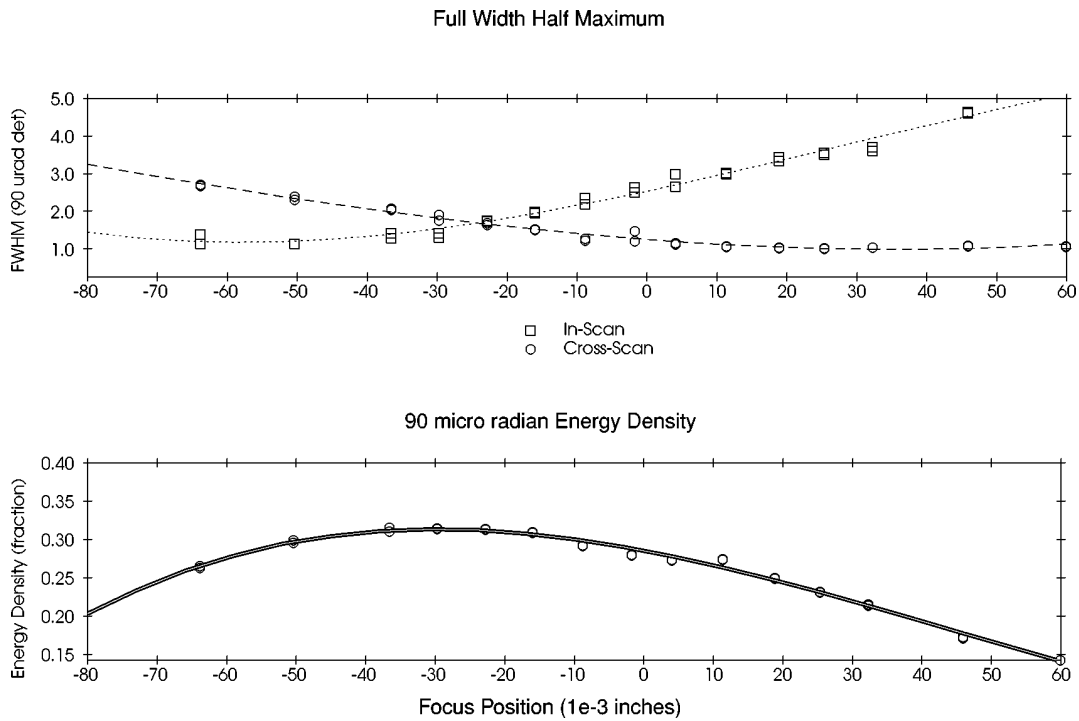


Fig. 6 Example focus test point response function figures of merit versus focus position.

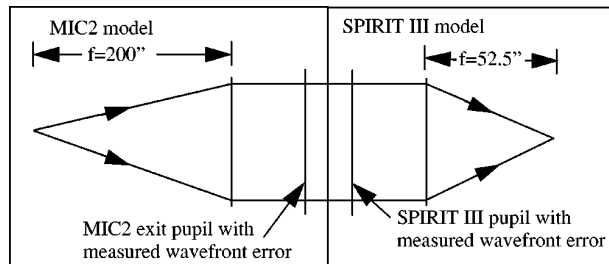


Fig. 7 Ray trace schematic of MIC2 and SPIRIT III optical model.

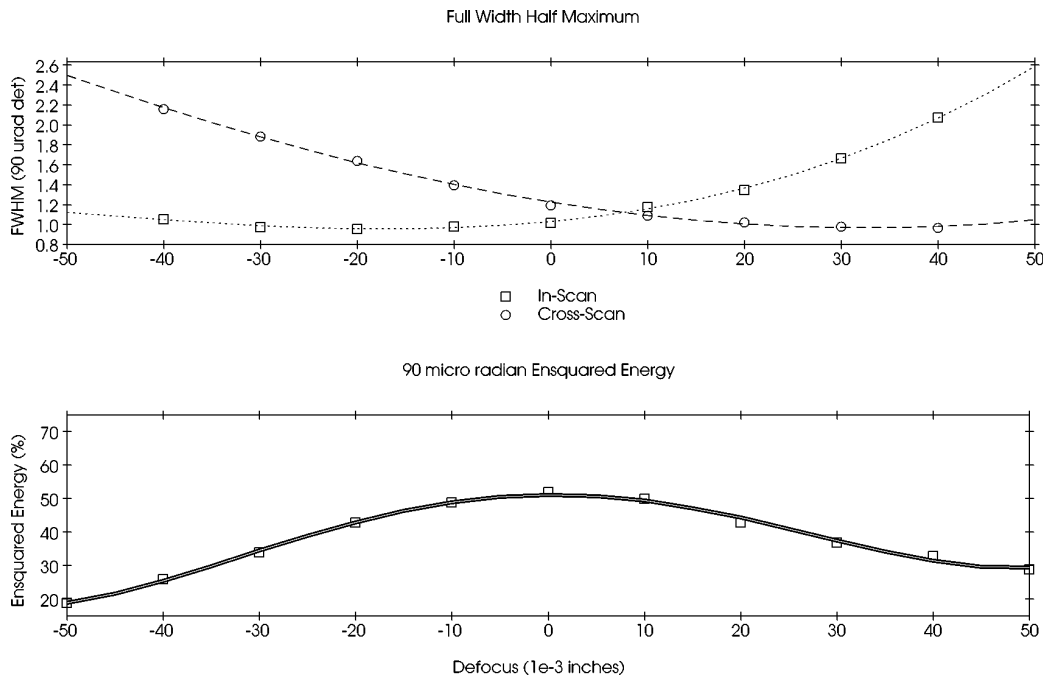


Fig. 8 Figure of merit results of SPIRIT III/MIC2 model ($\lambda = 12 \mu\text{m}$).

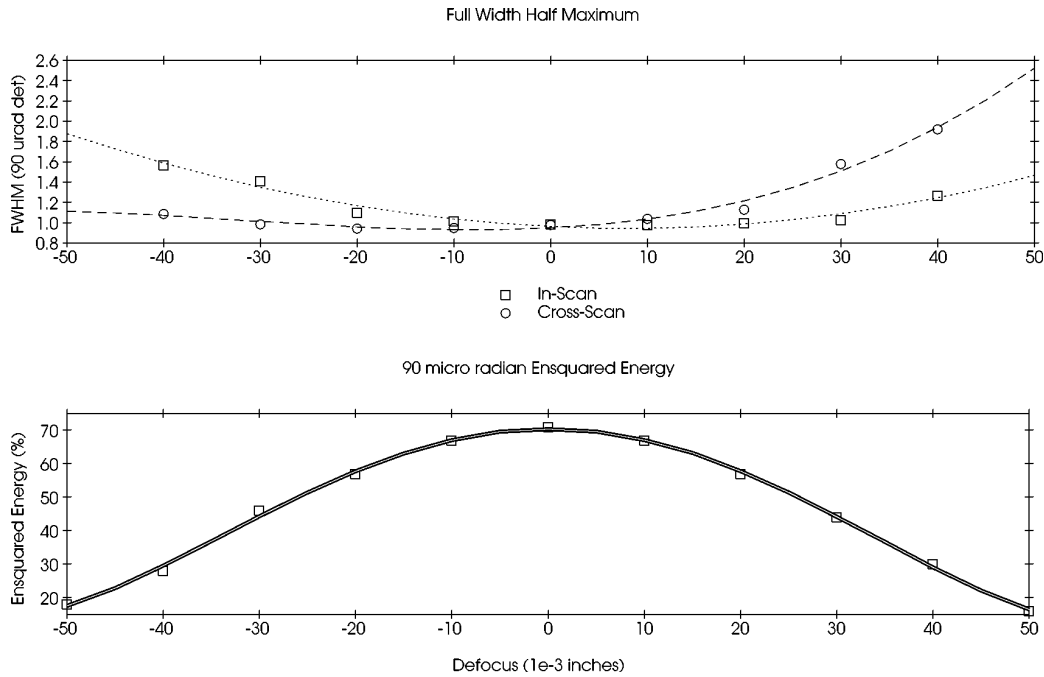


Fig. 9 Figure of merit results of SPIRIT III model for ideal point source ($\lambda = 12 \mu\text{m}$).

focus adjustment of only colocated arrays; hence, the optimum focus was then determined by averaging the optimal focus position of colocated arrays. Table 1 shows the implemented focus adjustment for each of the colocated arrays.

5 On-Orbit PRF

The on-orbit PRFs were measured by observing the star α Bootis near the center of the radiometer field of regard.¹⁰ Figure 10 shows an example of the on-orbit PRF for array C. This PRF is nearly symmetrical and has a 90- μrad ensquared energy of 69%. The on-orbit PRFs for all arrays were nearly symmetrical, demonstrating the success of this ground-based focus optimization technique.

6 Summary

Ground-based focus measurements were used to optimize the focus of the SPIRIT III radiometer. These measurements were obtained with a calibration source consisting of an illuminated pinhole near the focus of a cryogenic collimator. Simulated point source measurements were obtained at multiple focus positions by translating the pinhole along the optical axis inside and outside the optimum focus of the collimator. The radiometer PRF was measured at each focus position. The FWHM and 90- μrad energy density of the PRFs were calculated and plotted as a function of focus

position. The optimum focus of FWHM (i.e., symmetry) was found to be optimized at a slightly different focus position than the peak 90- μrad energy density. Because the optical model suggested that the MIC2 image quality biased the focus position determined by PRF symmetry, radiometer focus was optimized using the 90- μrad energy density figure of merit. This method employed a single cryogenic cycle to measure both the distance and direction needed to adjust each array for optimal focus. The nearly symmetrical character of the on-orbit stellar point source measurements substantiates the success of this technique.

Table 1 Radiometer focus adjustments.

Arrays	Focus Adjustment (in.)	Direction
A and B	0.017	Away from optics
C and D	0.035	Away from optics
E	0.032	Away from optics

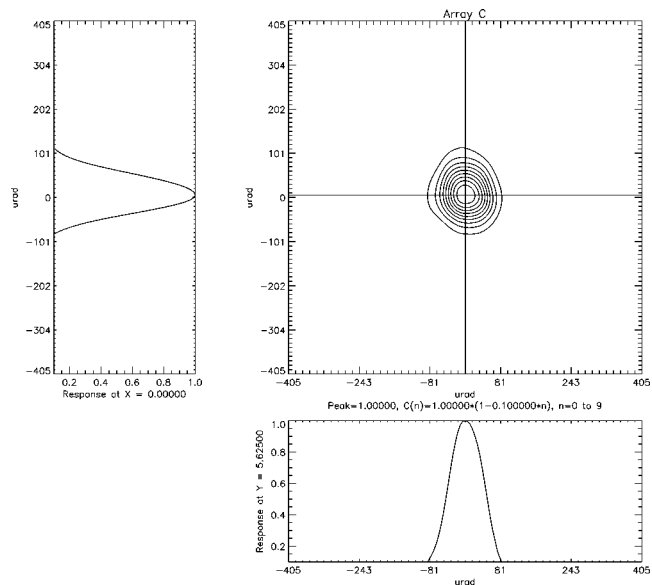


Fig. 10 Example on-orbit PRF for array C.

Acknowledgments

This work was sponsored by the Ballistic Missile Defense Organization, (BMDO). The authors gratefully acknowledge the support of BMDO and the MSX program. The authors also wish to acknowledge Roy Esplin, Alan Thurgood, Steve Sargent, and Harry Ames (SPIRIT III program manager) of SDL/USU for their expertise and technical assistance, Dave Pollock of the University of Alabama in Huntsville for his input from the Data Certification and Technology Transfer (DCATT) committee, and Dexter Wang of the Sensor Systems Group (SSG) for his expertise and technical assistance.

References

1. J. D. Mill, R. R. O'Neil, S. Price, G. J. Romick, O. M. Uy, E. M. Gaposchkin, G. C. Light, W. W. Moore, Jr., T. L. Murdock, and A. T. Stair, Jr., "Midcourse Space Experiment: introduction to the spacecraft, instruments, and scientific objectives," *J. Spacecraft Rock.* **31**(5), 900-907 (1994).
2. "SPIRIT III sensor user's guide," Space Dynamics Laboratory, Utah State University, SDL/92-041 (1995).
3. J. Blakeley, "Improved IR sensor characterizations using SDL/USU multifunction infrared calibrators," in Proc. 6th SDL/USU Symp. on Infrared Radiometric Sensor Calibration (1996).
4. C. L. Wyatt, L. Jacobsen, and A. Steed, "Portable compact multifunction IR calibrator," *Proc. SPIE* **940**, 63-72 (1988).
5. J. Tansock, A. Thurgood, and R. Esplin, "Focus optimization of a cryogenic collimator using interferometric measurements and optical modeling," *Proc. SPIE* **2268**, 196-206 (1994).
6. "SPIRIT III Convert User's Manual," Space Dynamics Laboratory, Utah State University, SDL/92-129 (1996).
7. *OSLO Series 2 and 3 Operating Manual*, Sinclair Optics, Inc., Fairport, NY (1991).
8. G. W. Willey and R. J. Patchin, "Optical design analysis incorporating actual system interferometric data," *Opt. Eng.* **32**(2), 401-409 (1993).
9. "Acceptance test procedure for SPIRIT III telescope," SSG, Inc., Waltham, MA (1991).
10. "SPIRIT III integrated ground and on-orbit calibration report in support of Convert 3.2," Space Dynamics Laboratory, Utah State University, SDL/96-042 (1996).

Joseph J. Tansock: Biography and photograph appear with the paper "SPIRIT III radiometer saturation effect" in this issue.



Andrew L. Shumway is a mechanical engineer with the Space Dynamics Laboratory at Utah State University. He specializes in the design, operation, and characterization of cryogenic optical-mechanical chambers used for calibrating IR sensors and has designed and characterized IR sources used as calibration standards. He received a BS in mechanical engineering from Brigham Young University in 1989 and an MS in mechanical and aerospace engineering from Utah State University in 1992. Mr. Shumway has also worked with engineering teams from the Planetary Society and Centre National d'Etudes Spatiales in Toulouse, France, to design systems for the exploration of Mars.